A&A 411, 559–564 (2003)
DOI: 10.1051/0004-6361:20031378

Astronomy & Astrophysics

High precision effective temperatures for 181 F–K dwarfs from line-depth ratios⋆,⋆⋆

V. V. Kovtyukh[1], C. Soubiran[2], S. I. Belik[1], and N. I. Gorlova[3]

[1] Astronomical Observatory of Odessa National University and Isaac Newton Institute of Chile, Shevchenko Park, 65014 Odessa, Ukraine
[2] Observatoire de Bordeaux, CNRS UMR 5804, BP 89, 33270 Floirac, France
[3] Steward Observatory, The University of Arizona, Tucson, AZ 85721, USA

Received 6 May 2003 / Accepted 19 August 2003

Abstract. Line depth ratios measured on high resolution ($R = 42\,000$), high S/N echelle spectra are used for the determination of precise effective temperatures of 181 F, G, K Main Sequence stars with about solar metallicity ($-0.5 <$ [Fe/H] $< +0.5$). A set of 105 relations is obtained which rely $T_{\rm eff}$ on ratios of the strengths of lines with high and low excitation potentials, calibrated against previously published precise (one per cent) temperature estimates. The application range of the calibrations is 4000–6150 K (F8V–K7V). The internal error of a single calibration is less than 100 K, while the combination of all calibrations for a spectrum of $S/N = 100$ reduces uncertainty to only 5–10 K, and for $S/N = 200$ or higher – to better than 5 K. The zero point of the temperature scale is directly defined from reflection spectra of the Sun with an uncertainty about 1 K. The application of this method to investigation of the planet host stars properties is discussed.

Key words. stars: fundamental parameters – stars: planetary systems

1. Introduction

The determination of accurate effective temperatures is a necessary prerequisite for detailed abundance analysis. In this paper we focus on dwarfs with solar metallicity ($-0.5 <$ [Fe/H] $< +0.5$) to contribute to the very active research field concerning the fundamental parameters of stars with planets. High precision temperatures of such stars might help to resolve two outstanding questions in the extra-solar planetary search. Namely, to get a definite confirmation of the metal richness of the stars that harbor planets, and secondly, perhaps to rule out some low-mass planetary candidates by detecting subtle variations in the host's temperature due to star-spots. The numerous studies of the large fraction of the known extra-solar planet hosts (~80 out of ~100 known systems) have revealed their larger than average metal richness (Gonzalez 1997; Fuhrmann et al. 1998; Gonzalez et al. 2001 and references therein; Takeda et al 2001; Santos et al. 2003 and references therein). The reliability of this result depends mainly on the accuracy of the model atmosphere parameters, with effective temperature ($T_{\rm eff}$) being the most important one.

The direct method to determine the effective temperature of a star relies on the measurement of its angular diameter and bolometric flux. In practice certain limitations restrict the use of this fundamental method to very few dwarfs. Other methods of temperature determination have errors of the order 50–150 K, which translates into the [Fe/H] error of ~0.1 dex or larger. The only technique capable so far of increasing this precision by one order of magnitude, is the one employing ratios of lines with different excitation potentials χ. As is well known, the lines of low and high χ respond differently to the change in $T_{\rm eff}$. Therefore, the ratio of their depths $r = R_{\lambda 1}/R_{\lambda 2}$ (or equivalent widths, EW) should be very sensitive temperature indicator. The big advantage of using line-depth ratios is the independence on the interstellar reddening, spectral resolution, rotational and microturbulence broadening.

The reader is referred to Gray (1989, 1994) and Gray & Johanson (1991) to learn more about the history and justification of the line ratio method. Applying this method to the Main-Sequence (MS) stars, they achieved precision as high as 10 K. The most recent works on the subject are by Caccin et al. (2002) who discuss the possible weak points of this technique for the case of dwarfs (see below), and the fundamental contribution by Strassmeier & Schordan (2000) who report 12 temperature calibrations for giants with an error of only 33 K.

So far however the line-ratio method has not been fully utilized for purposes other than just temperature estimation by itself. One of few applications is the chemical abundance

Send offprint requests to: V. V. Kovtyukh,
e-mail: val@deneb.odessa.ua

⋆ Based on spectra collected with the ELODIE spectrograph at the 1.93-m telescope of the Observatoire de Haute Provence (France).

⋆⋆ Full Table 1 is only available in electronic form at http://www.edpsciences.org

analysis of supergiants, where it has proved the anticipated high efficiency and accuracy. Thus, Kovtyukh & Gorlova (2000, hereafter Paper I) using high-dispersion spectra, established 37 calibrations for the temperature determination in supergiants (a further study increased this number to 55 calibrations). Based on this technique, in a series of 3 papers, Andrievsky et al. (2002, and references therein) derived temperatures for 116 Cepheids (from about 260 spectra) at a wide range of galactocentric distances (R_g = 5−15 kpc) with a typical error 5–20 K. The high precision of this new method of temperature determination allowed them to uncover the fine structure in the Galactic abundance gradients for many elements. Even for the most distant and faint objects ($V \simeq 13-14$ mag) the mean error in $T_{\rm eff}$ was no larger than 50–100 K, with maximum of 200 K for spectra with lowest S/N (= 40−50).

Another example concerns T Tau stars. For young stars, uncertainties in reddening due to variable circumstellar extinction invalidate the photometric color method of effective temperature determination. Using 5 ratios of FeI and VI lines calibrated against 13 spectral standards, Padgett (1996) determined the effective temperature of 30 T Tau stars with a 1 σ uncertainty lower than 200 K.

The intent of this paper is to improve this technique, based on our experience of applying it to supergiants (Paper I and following publications), and expand it to the MS stars. The wide spectral range of ELODIE echelle spectra allowed to select many unblended lines of low and high excitation potentials thus improving the internal consistency of the method, whereas the large intersection between the ELODIE database and published catalogues of effective temperatures allowed to take care of systematic effects. We obtained a median precision of 6 K on $T_{\rm eff}$ derived for an individual star. The zero-point of the scale was directly adjusted to the Sun, based on 11 solar reflection spectra taken with ELODIE, leading to the uncertainty in the zero-point of about 1 K.

Temperature determined by the line ratio method may now be considered as one of the few fundamental stellar parameters that have been measured with an internal precision of better than 0.2%.

2. Observations and temperature calibrations

The investigated spectra are part of the library collected with the ELODIE spectrometer on the 1.93-m telescope at the Haute-Provence Observatory (Soubiran et al. 1998; Prugniel & Soubiran 2001). The spectral range is 4400–6800 Å and the resolution is R = 42 000. The initial data reduction is described in Katz et al. (1998). All the spectra are parametrized in terms of $T_{\rm eff}$, $\log g$, [Fe/H], either collected from the literature or estimated with the automated procedure TGMET (Katz et al. 1998). This allowed us to select a sample of spectra of FGK dwarfs in the metallicity range $-0.5 <$ [Fe/H] $< +0.5$. Accurate Hipparcos parallaxes are available for all of the stars of interest enabling to determine their absolute magnitudes M_V that range between 2.945 (HD 81809, G2V) and 8.228 (HD 201092, K7V). All the selected spectra have a signal to noise ratio greater than 100 (see Fig. 1). Further processing of spectra (continuum placement, measuring equivalent

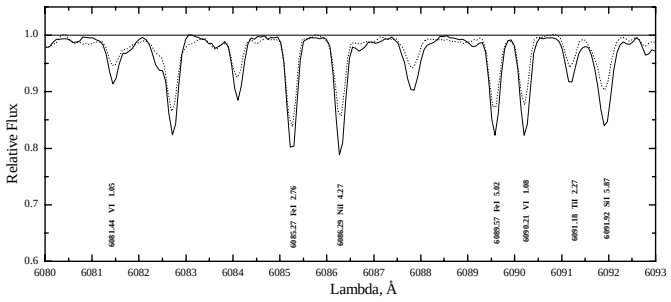

Fig. 1. Comparison spectra for two stars: *solid line* – a planet-host star HD 217014 (51 Peg), and *dotted line* – a non-planet star HD 5294. Within the limits of the errors, both stars have identical temperatures (5778 and 5779 K, respectively), but different metallicities. Spectral lines used in temperature calibrations are identified at the bottom with their wavelength, element, and lower excitation potentials χ in eV. We used ratios 6081.44/6089.57, 6085.27/6086.29, 6085.27/6155.14, 6089.57/6126.22, 6090.21/6091.92, 6090.21/6102.18, 6091.92/6111.65 and others.

widths, etc.) was carried out by us using the DECH20 software (Galazutdinov 1992). Equivalent widths EWs and depths R_λ of lines were measured manually by means of a Gaussian fitting. The Gaussian height was then a measure of the line depth. This method produces line depths values that agree nicely with the parabola technique adopted in Gray (1994). We refer the reader to Gray (1994, and references therein) and Strassmeier & Schordan (2000) for a detailed analysis of error statistics.

Following Caccin's et al. (2002) results, where a careful analysis of the anticipated problems for the Solar-type stars has been carried out, we did not use ion lines and high-ionization elements (like C, N, O) due to their strong sensitivity to gravity.

Gray (1994) showed that the ratio of lines VI 6251.82 and FeI 6252.55 depends strongly on metallicity. The reason is that the strong lines like FeI 6252.55 (R_λ = 0.52 for the Sun) are already in the dumping regime, where the linearity of EW on abundance breaks down. In addition, as was shown in the careful numerical simulations by Stift & Strassmeier (1995), this ratio (of 6251.82 and 6252.55 lines) is also sensitive to rotational broadening. Significant effects were found for $v \sin i$ as small as 0–6 km s^{-1} (for solar-like stars). We therefore avoided using strong lines in our calibrations. Indeed, Gray (1994) concluded that, as expected, the weak-line ratios are free from the effects of metallicity. As to the effect of rotation, we should note that all objects in our sample are old Main Sequence stars with slow to negligible rotation ($v \sin i < 15$ km s^{-1}), which is comparable to the instrumental broadening.

Thus, we initially selected about 600 pairs of 256 unblended SiI, TiI, VI, CrI, FeI, NiI lines with high and low excitation potentials within the wavelength interval 5300–6800 Å.

These lines have been selected according to the following criteria:

(1) the excitation potentials of the lines in a pair must differ as much as possible;

(2) the lines must be close in wavelength; it turned out though that calibrations based on widely spaced lines (including from different orders) show same small dispersion as the

Table 1. Program stars. Asterisks indicate stars with planets.

HD/BD	HR	Name	$T_{\rm eff}$ this paper	N	σ, K	$T_{\rm eff}$ EDV93	$T_{\rm eff}$ AAMR96	$T_{\rm eff}$ BLG98	$T_{\rm eff}$ DB98	Mv	$B-V$	rem
1562	–		5828	97	5.8					5.006	0.585	
1835	88	9 Cet	5790	68	5.5			5713	5774	4.842	0.621	
3765	–		5079	87	4.7					6.161	0.954	
4307	203	18 Cet	5889	91	5.0	5809	5753		5771	3.637	0.568	
4614	219	24 Eta Cas	5965	69	6.4	5946	5817			4.588	0.530	
5294	–		5779	86	6.6					5.065	0.610	
6715	–		5652	97	6.7					5.079	0.658	
8574	–		6028	61	6.7					3.981	0.535	*

closely spaced lines. Therefore, we retained all pairs with a difference in wavelength up to 70 Å ($\lambda_2 - \lambda_1 < 70$ Å);

(3) the lines must be weak enough to eliminate a possible dependence on microturbulence, rotation and metallicity;

(4) the lines must be situated in the spectral regions free from telluric absorption.

The next step was to choose the initial temperatures for interpolation. This is a very important procedure since it affects the accuracy of the final temperature scale, namely, the run of the systematic error with $T_{\rm eff}$ (Fig. 3). There is an extended literature on MS stars temperatures. For 45 stars from our sample (see Table 1) we based the initial temperature estimates on the following 3 papers: Alonso et al. (1996, hereafter AAMR96), Blackwell & Lynas–Gray (1998, hereafter BLG98) and DiBenedetto (1998, hereafter DB98). In these works the temperatures have been determined for a large fraction of stars from our sample with a precision of about 1%. AAMR96 used the Infrared Flux Method (IRFM) to determine $T_{\rm eff}$ for 475 dwarfs and subdwarfs with a mean accuracy of about 1.5% (i.e., 75–90 K). BLG98 also have determined temperatures for 420 stars with spectral types between A0 and K3 by using IRFM and achieved an accuracy of 0.9%. DB98 derived $T_{\rm eff}$ for 537 dwarfs and giants by the empirical method of surface brightness and Johnson broadband ($V-K$) color, the accuracy claimed is ±1%. Whenever 2 or 3 estimates were available for a given star, we averaged them with equal weights. These temperatures served as the initial approximations for our calibrations.

First, for the mentioned above 45 stars with previously accurately determined $T_{\rm eff}$ we plotted each line ratio against $T_{\rm eff}$, and retained only those pairs of lines that showed unambiguous and tight correlation. We experimented with a total of nearly 600 line ratios but adopted only the 105 best – the ones showing the least scatter. These 105 calibrations consist of 92 lines, 45 with low ($\chi < 2.77$ eV) and 47 with high ($\chi > 4.08$ eV) excitation potentials. Judging by the small scatter in our final calibrations (Fig. 2) and $T_{\rm eff}$, the selected combinations are only weakly sensitive to effects like rotation, metallicity and microturbulence. This confidence is reinforced by the fact that the employed lines belong to a wide range of chemical elements, intensity and atomic parameters, therefore one can expect the mutual cancellation of opposite effects.

Each relationship was then fitted with a simple analytical function. Often calibrations show breaks which not can be adequately described even by a 5th-order polynomial function (see Fig. 2). Therefore, we employed other functions as well, like the Hoerl function ($T_{\rm eff} = ab^r * r^c$, where $r = R_{\lambda1}/R_{\lambda2}$, a, b, c – constants), modified Hoerl ($T_{\rm eff} = ab^{1/r}r^c$), power low ($T_{\rm eff} = ar^b$), exponential ($T_{\rm eff} = ab^r$) and logarithmic ($T_{\rm eff} = a+b\ ln(r)$) functions. For each calibration we selected the function that produced the least square deviation. As a result, we managed to accurately approximate the observed relationships with a small set of analytic expressions. This first step allowed us to select 105 combinations, with an rms of the fit lower than 130 K, the median rms being 93 K. Using these initial rough calibrations, for each of the 181 target stars we derived a set of temperatures (70–100 values, depending on the number of line ratios used), averaged them with equal weights, and plotted these mean $T_{\rm eff}$ (with errors of only 10–20 K) versus line ratios again, thus determining the preliminary calibrations (for which the zero-point had yet to be adjusted).

We would like to point out that the precision of our calibrations varies with temperature. In particular, at high $T_{\rm eff}$ the lines with low χ become very weak causing the line depth measurement to be highly uncertain. Therefore, for each calibration we determined the optimum temperature range where the maximum accuracy is attained (no worse than 100 K), so that for a given star only a subset of calibrations can be applied.

What are the main sources of random errors in the line ratio method? The measurement errors in line depths are mainly caused by the continuum placement uncertainty and by the Gaussian approximation of the line profile. In addition, the individual properties of the stars, such as metallicity, spots, rotation, convection, non-LTE effects and binarity may also be responsible for the scatter observable in Fig. 2. The detailed analysis of these and other effects can be found in Paper I, Strassmeier & Schordan (2000) and in works by D. F. Gray. We estimate that the typical error in the line depth measurement $r = R_{\lambda1}/R_{\lambda2}$ is 0.02−0.05, implying an error in temperature of about 20–50 K.

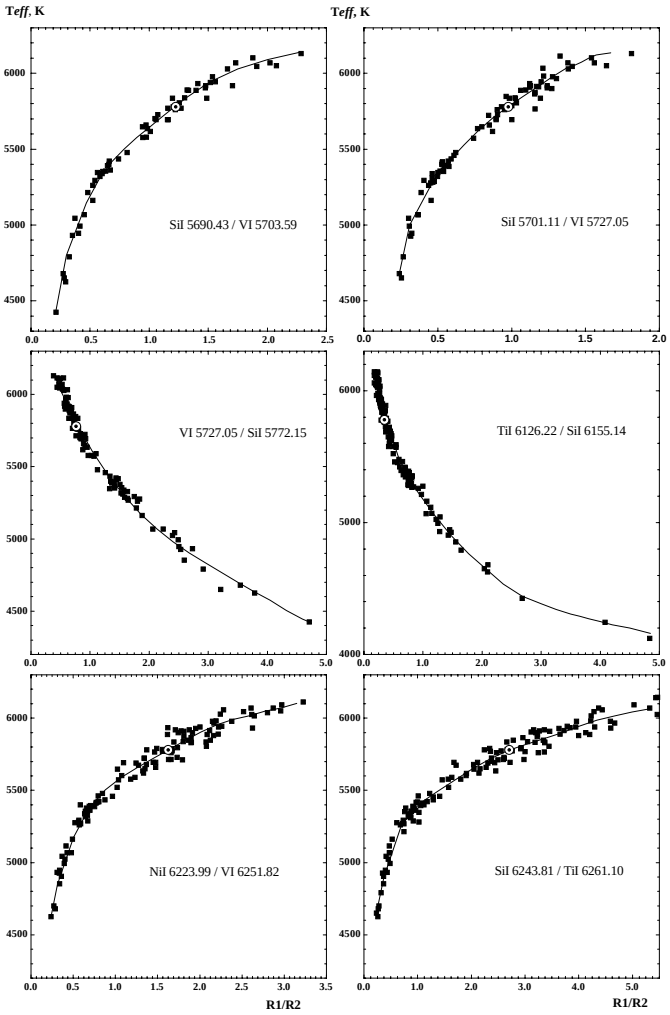

Fig. 2. Our final calibrations of temperature versus line depth ratios $r = R1/R2$. The temperatures are shown as the average value derived from all calibrations available for a given star. The errors in temperature are less than the symbol size. The typical error in line ratio is 0.02–0.05. Position of the Sun is marked by the standard symbol.

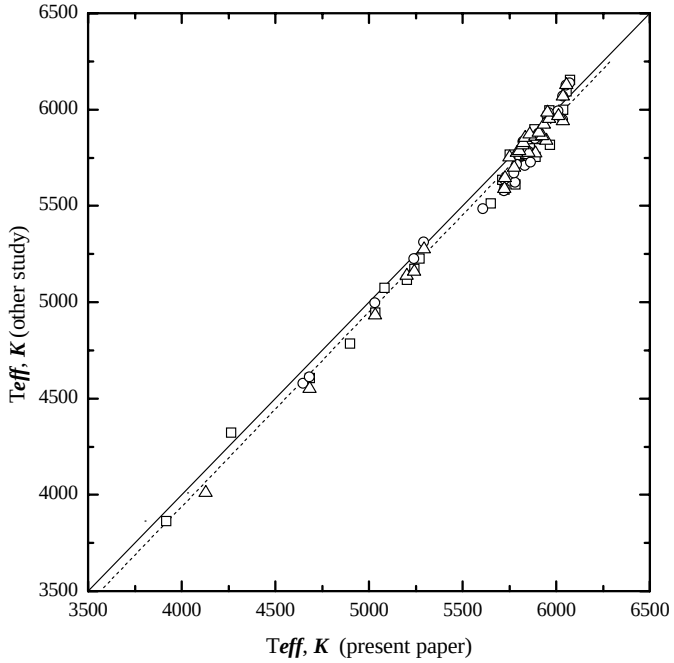

Fig. 3. Comparison between the temperatures derived in the present work and those derived by AAMR96 – *squares*, BLG98 – *circles*, and DB98 – *triangles*. The dashed line represents the linear fit to the data, and the solid line represents the one-to-one correlation.

The mean random error of a single calibration is 60–70 K (40–45 K in the most and 90–95 K in the least accurate cases). The use of ~70–100 calibrations reduces the uncertainty to 5–7 K (for spectra with $S/N = 100-150$). Better quality spectra ($R > 100\,000$, $S/N > 400$) should in principle allow an uncertainty of just 1–2 K. Clearly, time variation of the temperature for a given star should be readily detected by this method, since the main parameters that cause scatter due to star-to-star dissimilarities (gravity, rotation, [Fe/H], convection, non-LTE effects etc.) are fixed for a given star. The temperature variation of several degrees in mildly active stars may be produced by the surface features and rotational modulation, as for example has been documented for the G8 dwarf ξ Bootis A (Toner & Gray 1988) and σ Dra (K0V, Gray et al. 1992).

The next stage is to define the zero point of our temperature scale. Fortunately, for dwarfs (unlike for supergiants) a well-calibrated standard exists, the Sun. Using our preliminary calibrations and 11 independent solar spectra from the ELODIE library (reflection spectra of the Moon and asteroids), we obtained a mean value of 5733 ± 0.9 K for the Sun's temperature. Considering the Sun as a normal star, we adjusted our calibrations by adding 44 K to account for the offset between the canonical Solar temperature of 5777 K and our estimate. The possible reasons for this small discrepancy are discussed below.

3. Results and discussion

Table 1 contains our final $T_{\rm eff}$ determinations for 181 MS stars. Note that we added the 44 K correction to the initial calibrations in order to reproduce the standard 5777 K temperature of the Sun. For each star we report the mean $T_{\rm eff}$, number of the calibrations used (N), and the standard error of the mean (σ). For comparison, we also provide $T_{\rm eff}$ as determined in Edvardsson et al. (1993, hereafter EDV93), AAMR96, BLG98 and DB98. Absolute magnitudes M_V have been computed from Hipparcos parallaxes and V magnitudes from the Tycho2 catalogue (Høg et al. 2000) transformed into Johnson system. $(B-V)$ are also from Tycho2. Planet-harboring stars are marked with an asterisk.

As one can see from Table 1, for the majority of stars we get an error which is smaller than 10 K. The consistency of the results derived from the ratios of lines representing different elements is very reassuring. It shows that our 105 calibrations are essentially independent of micro-turbulence, LTE departures, abundances, rotation and other individual properties of stars. We admit though that a small systematic error may exist for $T_{\rm eff}$ below 5000 K where we had only few standard stars.

As was already mentioned, for the first approximation we took accurate temperatures from AAMR96, BLG98 and DB98.

Table 2. RMS of a linear regression between $T_{\rm eff}$ and Strömgren $b{-}y$ using effective temperatures obtained by other authors and in this study with N common stars.

author	N	$\sigma_{\rm others}$ K	$\sigma_{\rm our}$ K
AAMR96	30	102	78
BLG98	25	71	65
DB98	29	113	87
EDV93	30	63	29

The comparison of our final $T_{\rm eff}$ with those derived by AAMR96, BLG98 and DB98 is shown in Fig. 3. As a test of the internal precision of our $T_{\rm eff}$ we investigate the $T_{\rm eff}$ – color relation with the Strömgren index b–y, using our determinations of $T_{\rm eff}$, and those obtained by other authors. The results are shown in Table 2 where the rms of the linear fit is given for each author's determination, along with our estimate of $T_{\rm eff}$ and using common stars. In each case the scatter of the color relation is significantly improved when adopting our temperatures, though some residual dispersion is still present that can be attributed to the photometric errors, reddening and the intrinsic properties of stars (metallicity, gravity, binarity...) to which the color indices are known to be sensitive. The improvement is particulary spectacular in comparison with EDV93. This proves the high quality of our temperatures and the mediocrity of b–y as a temperature indicator.

Another point concerns the difference between the zero-point of our temperature scale and that of other authors. Comparing 30 common objects, we find that the AAMR96 scale underestimates temperatures by 45 K near the solar value compared to ours, but apart from that, the deviations are random and no trend with $T_{\rm eff}$ is present. The 45 K offset may arise from the various complications associated with observing the Sun as a star, and/or problems in the models used by AAMR96, like underestimation of convection in the grid of the model atmosphere flux developed by Kurucz. After correcting the AAMR96 zero-point for the 45 K offset, the mean random error of their scale becomes 65 K (where we neglect the error of our own scale which is an order of magnitude less).

The temperatures of BLG98 are also in a good agreement with our estimates – except for a 48 K offset, no correlation of the difference with temperature is observed. The mean dispersion is 63 K (for 26 common stars), which is within the errors of the BLG98 scale.

Comparing with DB98: for the 29 stars in common, their temperatures are on average 41 K below ours, and the mean error is ±53 K.

Thus, the temperatures derived in AAMR96, BLG98 and DB98 have good precision, though the absolute values are somewhat low relative to the Sun. The reason may be due to the difficulty of photometric measurements of the Sun, as well as indicating some problems in the model atmosphere calculations employed. For example, the Sun's temperatures derived in AAMR96 and DB98 are identical – 5763 K, which is below the nominal value of 5777 K. Besides, the mean temperatures of solar analogue stars (spectral types G2–G3, [Fe/H] ≈ 0.0, and Sun being of type G2.5) derived in these papers are significantly below the solar value: 5720 ± 54 K (AAMR96, 3 stars), 5692 ± 31 K (BLG98, 11 stars) and 5702 ± 46 K (DB98, 7 stars). Our determination for the G2–G3 spectral types is 5787 ± 14 K, based on 12 stars. This demonstrates that a small error (0.8%) affects the zero point of the IRFM method, because when applied to the Sun and the solar type stars, it returns inconsistent results.

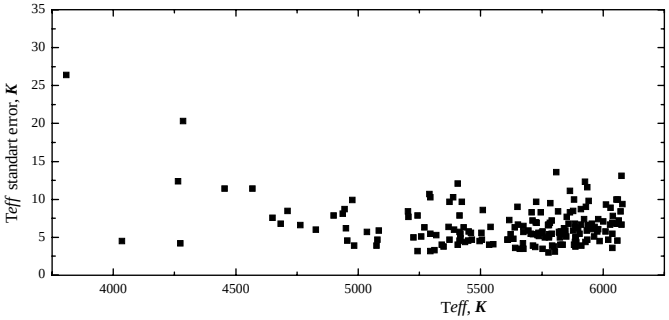

Fig. 4. Standard error of the mean versus effective temperature averaged over all available line ratios.

We also compared our estimates of $T_{\rm eff}$ with photometric temperatures. EDV93 derived temperatures of 189 nearby field F, G disk dwarfs using the theoretical calibration of temperature versus Strömgren (b–y) photometry (see Table 1). The mean difference between the $T_{\rm eff}$ of Edvardsson et al. (1993) and ours is only −14 K (σ = ±67 K, based on 30 common stars).

To compare our temperatures to Gray (1994), we used his calibration of $(B-V)_{\rm corr}$ corrected for metallicity. Our scale is +11 K lower (σ = ±61 K, 24 stars).

Summarizing, we demonstrated that our temperature scale is in excellent agreement with the widely used photometric scales, while both the IRFM method and the method of surface brightness predict too low values for the temperature of the Sun and the solar type stars.

Figure 4 shows the sensitivity of our technique to temperature. Two outliers with errors greater than 20 K are the cold dwarfs HD 28343 and HD 201092, known as flaring stars. For other stars the internal errors range between 3 and 13 K, with a median of 6 K.

4. Conclusion

The high-precision temperatures were derived for a set of 181 dwarfs, which may serve as temperature standards in the 4000–6150 K range. These temperatures are precise to within 3–13 K (median 6 K) for the major fraction of the sample, except for the two outliers. We demonstrated that the line ratio technique is capable of detecting variations in $T_{\rm eff}$ of a given star as small as 1–5 K. This precision may be enough to detect star spots and Solar-type activity cycles. Of particular interest is the application of this method to testing ambiguous cases of low-mass planet detection, since planets do not cause temperature variations, unlike spots.

The next step will be the adaptation of this method to a wider range of spectral types and for an automatic pipeline analysis of large spectral databases.

Acknowledgements. V.K. wants to thank the staff of Observatoire de Bordeaux for the kind hospitality during his stay there. The authors are also grateful to the anonymous referee for the careful reading of the manuscript and the numerous important remarks that helped to improve the paper.

References

Alonso, A., Arribas, S., & Martínez-Roger, C. 1996, A&AS, 117, 227 (AAMR96)
Andrievsky, S. M., Kovtyukh, V. V., Luck, R. E., et al. 2002, A&A, 392, 491
Blackwell, D. E., & Lynas–Gray, A. E. 1998, A&AS, 129, 505 (BLG98)
Caccin, B., Penza, V., & Gomez, M. T. 2002, A&A, 386, 286
Di Benedetto, G. P. 1998, A&A, 339, 858 (DB98)
Edvardson, B., Andersen, J., Gustafsson, B., et al. 1993, A&A, 275, 101 (EDV93)
Fuhrmann, K., Pfeiffer, M. J., & Bernkopf, J. 1998, A&A, 336, 942
Galazutdinov, G. A. 1992, Preprint SAO RAS, 28
Gonzalez, G. 1997, MNRAS, 285, 403
Gonzalez, G., Laws, C., Tyagi, S., & Reddy, B. E. 2001, AJ, 121, 432
Gray, D. F. 1989, ApJ, 347, 1021
Gray, D. F. 1994, PASP, 106, 1248
Gray, D. F., & Johanson, H. L. 1991, PASP, 103, 439
Gray, D. F., Baliunas, S. L., Lockwood, G. W., & Skiff, B. A. 1992, ApJ, 400, 681
Høg, E., Fabricius, C., Makarov, V. V., et al. 2000, A&A, 355, L27
Katz, D., Soubiran, C., Cayrel, R., Adda, M., & Cautain, R. 1998, A&A, 338, 151
Kovtyukh, V. V., & Gorlova, N. I. 2000, A&A, 358, 587
Padgett, D. L. 1996, ApJ, 471, 847
Prugniel, P., & Soubiran, C. 2001, A&A, 369, 1048
Santos, N. C., Israelian, G., Mayor, M., Rebolo, R., & Udry, S. 2003, A&A, 398, 363
Soubiran, C., Katz, D., & Cayrel, R. 1998, A&AS, 133, 221
Stift, M. J., & Strassmeier, K. G. 1995, in Stellar Surface Structure, Poster Proc, ed. K. G. Strassmeier, IAU Symp. 176, Univ. Vienna, 29
Strassmeier, K. G., & Schordan, P. 2000, AN, 321, 277
Takeda, Y., Sato, B., Kambe, E., Aoki, W., et al. 2001, PASJ, 53, 1211
Toner, C. G., & Gray, D. F. 1988, ApJ, 334, 1008

Online Material

Table 1. Program stars. Asterisks indicate stars with planets.

HD	HR	Name	$T_{\rm eff}$ this paper	N	σ, K	$T_{\rm eff}$ EDV93	$T_{\rm eff}$ AAMR96	$T_{\rm eff}$ BLG98	$T_{\rm eff}$ DB98	Mv	$B-V$	rem
1562	–		5828	97	5.8					5.006	0.585	
1835	88	9 Cet	5790	68	5.5			5713	5774	4.842	0.621	
3765	–		5079	87	4.7					6.161	0.954	
4307	203	18 Cet	5889	91	5.0	5809	5753		5771	3.637	0.568	
4614	219	24 Eta Cas	5965	69	6.4	5946	5817			4.588	0.530	
5294	–		5779	86	6.6					5.065	0.610	
6715	–		5652	97	6.7					5.079	0.658	
8574	–		6028	61	6.7					3.981	0.535	*
8648	–		5790	59	7.2					4.421	0.643	
9826	458	50 Ups And	6074	44	13.1	6212	6155	6136		3.452	0.496	*
10145	–		5673	96	4.2					4.871	0.667	
10307	483		5881	94	4.0	5898	5874			4.457	0.575	
10476	493	107 Psc	5242	69	3.2		5172	5223	5157	5.884	0.819	
10780	511		5407	95	4.0					5.634	0.767	
11007	523		5980	84	7.4					3.612	0.524	
13403	–		5724	91	7.0		5585	5577	5588	3.949	0.616	
13507	–		5714	91	5.4					5.123	0.637	*
13825	–		5705	96	5.5					4.700	0.674	
14374	–		5449	77	4.6					5.492	0.757	
15335	720	13 Tri	5937	84	6.6	5857			5921	3.468	0.539	
17674	–		5909	58	8.7			5875	5880	4.194	0.563	
17925	857		5225	87	5.0					5.972	0.864	
18803	–		5659	95	3.5					4.998	0.669	
19019	–		6063	56	7.2					4.445	0.508	
19308	–		5844	95	5.4					4.220	0.626	
19373	937	Iot Per	5963	75	5.1		5996	5981	5951	3.935	0.554	
19994	962	94 Cet	6055	56	10.0	6104				3.313	0.523	*
22049	1084	18 Eps Eri	5084	84	5.9		5076			6.183	0.877	*
22484	1101	10 Tau	6037	60	3.6	5981	5998	5944	5940	3.610	0.527	
23050	–		5929	80	9.0					4.330	0.544	
24053	–		5723	93	3.7					5.183	0.674	
24206	–		5633	94	4.8					5.418	0.681	
26923	1322	V774 Tau	5933	77	5.9					4.685	0.537	
28005	–		5980	87	6.1					4.359	0.652	
28099	–		5778	85	5.2					4.747	0.660	
28343	–		4284	20	20.3					8.055	1.363	
28447	–		5639	93	6.3					3.529	0.678	
29150	–		5733	89	5.4					4.934	0.668	
29310	–		5852	89	7.7			5781	5775	4.407	0.564	
29645	1489		6009	57	5.8	6028				3.504	0.548	
29697	–		4454	40	11.4					7.483	1.108	
30495	1532	58 Eri	5820	91	5.7					4.874	0.588	
30562	1536		5859	87	6.8	5886	5822	5843	5871	3.656	0.593	
32147	1614		4945	65	8.7					6.506	1.077	
34411	1729	15 Lam Aur	5890	88	4.3	5889	5847	5848	5859	4.190	0.575	
38858	2007		5776	81	6.7			5669	5697	5.014	0.584	
39587	2047	54 Chi1 Ori	5955	71	6.1	5953				4.716	0.545	
40616	–		5881	89	10.0					3.833	0.585	
41330	2141		5904	77	5.5	5917				4.021	0.547	
41593	–		5312	92	3.3					5.814	0.802	
42618	–		5775	96	6.6					5.053	0.603	
42807	2208		5737	81	5.2					5.144	0.631	
43587	2251		5927	81	4.4					4.280	0.558	
43947	–		6001	82	7.1	5945				4.426	0.507	
45067	2313		6058	61	4.6					3.278	0.507	
47309	–		5791	95	3.9					4.469	0.623	
50281	–		4712	56	8.5					6.893	1.074	
50554	–		5977	77	5.8					4.397	0.529	*
51419	–		5746	94	8.3					5.013	0.600	
55575	2721		5949	65	6.6	5963			5839	4.418	0.531	
58595	–		5707	87	8.3					5.105	0.665	

Table 1. continued.

HD	HR	Name	$T_{\rm eff}$ this paper	N	σ, K	$T_{\rm eff}$ EDV93	$T_{\rm eff}$ AAMR96	$T_{\rm eff}$ BLG98	$T_{\rm eff}$ DB98	Mv	$B-V$	rem
60408	–		5463	97	4.7					3.100	0.760	
61606	–		4956	83	4.6					6.434	0.955	
62613	2997		5541	90	6.4					5.398	0.695	
64815	–		5864	88	8.3					3.375	0.605	
65874	–		5936	85	4.7					3.100	0.574	
68017	–		5651	100	9.0		5512			5.108	0.630	
68638	–		5430	90	6.3					5.021	0.746	
70923	–		5986	82	4.5					3.879	0.556	
71148	3309		5850	88	5.1					4.637	0.587	
72760	–		5349	91	3.8					5.628	0.796	
72905	3391	3 Pi1 UMa	5884	79	6.8					4.869	0.573	
73344	–		6060	37	6.8					4.169	0.515	
75318	–		5450	78	5.8					5.345	0.717	
75732	3522	55 Rho1 Cnc	5373	97	9.7					5.456	0.851	*
76151	3538		5776	88	3.0	5763				4.838	0.632	
76780	–		5761	87	5.0					5.011	0.648	
81809	3750		5782	85	6.9		5611	5619		2.945	0.606	
82106	–		4827	76	6.0					6.709	1.000	
86728	3951	20 LMi	5735	91	5.6	5746				4.518	0.633	
88072	–		5778	82	5.0					4.717	0.593	
89251	–		5886	89	6.3					3.292	0.569	
89269	–		5674	95	5.7					5.089	0.645	
89389	4051		6031	48	8.9					4.034	0.532	
91347	–		5923	75	7.4					4.725	0.513	
95128	4277	47 UMa	5887	89	3.8	5882				4.299	0.576	*
96094	–		5936	73	11.6					3.725	0.550	
98630	–		6060	52	10.0					3.043	0.553	
99491	4414	83 Leo	5509	96	8.6					5.230	0.785	
101206	–		4649	60	7.6			4576		6.750	0.983	
102870	4540	5 Bet Vir	6055	48	6.8	6176	6095	6124	6127	3.407	0.516	
107705	4708	17 Vir	6040	56	7.8					4.104	0.498	
108954	4767		6037	60	5.5	6060		6068	6068	4.507	0.518	
109358	4785	8 Bet CVn	5897	72	6.2	5879	5867			4.637	0.549	
110833	–		5075	80	3.9					6.130	0.938	
110897	4845	10 CVn	5925	68	12.3	5795			5862	4.765	0.510	
112758	–		5203	83	8.4		5116		5137	5.931	0.791	
114710	4983	43 Bet Com	5954	71	6.8	6029	5964	5959	5985	4.438	0.546	
115383	5011	59 Vir	6012	40	9.3	6021		5989	5967	3.921	0.548	
116443	–		4976	83	9.9					6.175	0.850	
117043	5070		5610	98	4.7					4.851	0.729	
117176	5072	70 Vir	5611	104	4.7			5482		3.683	0.678	*
119802	–		4763	71	6.6					6.881	1.099	
122064	5256		4937	84	8.1					6.479	1.038	
122120	–		4568	35	11.4					7.148	1.176	
124292	–		5535	89	4.0					5.311	0.721	
125184	5353		5695	89	5.9	5562				3.898	0.699	
126053	5384		5728	79	6.9			5635	5645	5.032	0.600	
130322	–		5418	85	5.4					5.668	0.764	*
131977	5568		4683	62	6.8		4605	4609	4551	6.909	1.091	
135204	–		5413	91	4.6					5.398	0.742	
135599	–		5257	86	5.1					5.976	0.804	
137107	5727	2 Eta CrB	6037	60	6.9					4.237	0.507	
139323	–		5204	90	7.7					5.909	0.943	
139341	–		5242	90	7.9					5.115	0.898	
140538	5853	23 Psi Ser	5675	100	3.5					5.045	0.640	
141004	5868	27 Lam Ser	5884	81	4.4	5937	5897			4.072	0.558	
143761	5968	15 Rho CrB	5865	81	11.1	5782		5726		4.209	0.560	*
144287	–		5414	93	5.7					5.450	0.739	
144579	–		5294	89	10.3			5309	5275	5.873	0.707	
145675	–		5406	98	12.1					5.319	0.864	
146233	6060	18 Sco	5799	96	3.8					4.770	0.614	

Table 1. continued.

HD/BD	HR	Name	$T_{\rm eff}$ this paper	N	σ, K	$T_{\rm eff}$ EDV93	$T_{\rm eff}$ AAMR96	$T_{\rm eff}$ BLG98	$T_{\rm eff}$ DB98	Mv	$B-V$	rem
149661	6171	12 Oph	5294	90	3.2					5.817	0.817	
151541	–		5368	88	6.4					5.630	0.757	
152391	–		5495	82	4.5					5.512	0.732	
154345	–		5503	87	5.6					5.494	0.708	
154931	–		5910	82	6.7					3.558	0.578	
157214	6458	72 Her	5784	85	9.5	5676				4.588	0.572	
157881	–		4035	9	4.5				4011	8.118	1.371	
158614	6516		5641	98	3.6					4.910	0.678	
158633	6518		5290	83	10.7					5.896	0.737	
159062	–		5414	96	7.9					5.485	0.706	
159222	6538		5834	93	4.0		5770	5708	5852	4.653	0.617	
159909	–		5749	93	5.6					4.459	0.657	
160346	–		4983	84	3.9					6.382	0.950	
161098	–		5617	90	7.3					5.294	0.632	
164922	–		5392	96	6.0					5.293	0.789	
165173	–		5505	95	4.7					5.388	0.732	
165401	–		5877	85	8.5	5758				4.880	0.557	
165476	–		5845	90	5.9					4.406	0.580	
166620	6806		5035	75	5.7		4947	4995	4930	6.165	0.871	
168009	6847		5826	93	4.0		5781	5833	5826	4.528	0.596	
170512	–		6078	43	9.4					3.965	0.542	
171067	–		5674	81	6.5					5.191	0.660	
173701	–		5423	104	9.7					5.343	0.847	
176841	–		5841	92	6.2					4.487	0.637	
182488	7368		5435	82	4.4					5.413	0.788	
183341	–		5911	85	3.9					4.201	0.575	
184385	–		5552	87	4.1					5.354	0.721	
184768	–		5713	94	3.9					4.593	0.645	
185144	7462	61 Sig Dra	5271	79	6.3		5227			5.871	0.765	
186104	–		5753	95	5.8					4.621	0.631	
186379	–		5941	67	9.8					3.586	0.512	
186408	7503	16 Cyg A	5803	83	3.1		5763		5783	4.258	0.614	
186427	7504	16 Cyg B	5752	77	3.5		5767		5752	4.512	0.622	*
187123	–		5824	86	5.0					4.433	0.619	*
187897	–		5887	95	5.0					4.521	0.585	
189087	–		5341	83	4.0					5.873	0.782	
189340	7637		5816	90	8.4					3.920	0.532	
190067	–		5387	100	10.3					5.731	0.707	
195005	–		6075	51	6.7					4.302	0.498	
197076	7914		5821	75	5.6		5761	5774	5815	4.829	0.589	
199960	8041	11 Aqr	5878	78	5.9	5813				4.089	0.590	
201091	8085	61 Cyg	4264	17	12.4		4323			7.506	1.158	
201092	8086	61 Cyg	3808	5	26.4		3865			8.228	1.308	
202108	–		5712	82	7.2		5635			5.186	0.610	
203235	–		6071	52	8.4					3.606	0.468	
204521	–		5809	74	13.6					5.245	0.545	
205702	–		6020	50	4.7					3.839	0.513	
206374	–		5622	89	5.4					5.304	0.674	
210667	–		5461	81	5.6					5.470	0.800	
211472	–		5319	91	5.3					5.835	0.802	
215065	–		5726	95	9.7					5.131	0.594	
215704	–		5418	95	4.9					5.500	0.795	
217014	8729	51 Peg	5778	92	5.4	5755				4.529	0.615	*
219134	8832		4900	63	7.9		4785			6.494	1.009	
219396	–		5733	91	5.3					3.918	0.654	
220182	–		5372	94	4.7					5.661	0.788	
221354	–		5295	95	5.5					5.610	0.830	
+32 1561	–		4950	82	6.2					6.493	0.919	
+46 1635	–		4273	12	4.2					7.895	1.367	
Sun	–		5777	889	0.9					4.790	0.65	